European Journal of Nuclear Medicine and Molecular Imaging (2021) 48:1487–1497
https://doi.org/10.1007/s00259-020-05078-1

ORIGINAL ARTICLE

A proposed index of diffuse bone marrow [18F]-FDG uptake and PET skeletal patterns correlate with myeloma prognostic markers, plasma cell morphology, and response to therapy

A. Paschali[1] · E. Panagiotidis[1] · T. Triantafyllou[2] · V. Palaska[2] · K. Tsirou[2] · E. Verrou[2] · E. Yiannaki[3] · D. Markala[3] · A. Papanikolaou[4] · A. Pouli[5] · P. Konstantinidou[2] · V. Chatzipavlidou[1] · E. Terpos[6] · E. Katodritou[2]

Received: 10 September 2020 / Accepted: 15 October 2020 / Published online: 25 October 2020

Abstract

Purpose The investigation of a semi-quantitative index in the pelvis to assess for diffuse bone marrow (BM) [18F]-FDG uptake and the investigation of PET skeletal patterns in multiple myeloma (MM) patients, in accordance with prognostic markers, clonal plasma cell (cPC) morphology, and response to therapy.

Methods We prospectively analyzed [18F]-FDG PET/CT in 90 MM patients (newly diagnosed, 60; relapsed/refractory, 30). Among other PET/CT parameters, we calculated the ratio SUVmax pelvis/liver and examined for correlations with known MM prognostic parameters, cPC morphology (good vs. low/intermediate differentiation), and response to therapy.

Results SUVmax pelvis/liver ratio was significantly lower for the group of good differentiation vs. intermediate/low differentiation cPCs ($p < 0.001$) and showed a positive correlation with BM infiltration rate, β2 microglobulin, serum ferritin, international staging system (ISS), and revised ISS; no significant correlation was found with hemoglobin. A cutoff value of 1.1 showed an excellent specificity (99%) and high sensitivity (76%) for diffuse BM involvement (AUC 0.94; $p < 0.001$). Mixed pattern and appendicular involvement correlated with poor prognostic features while normal pattern, found in 30% of patients, correlated with good prognostic features. Presence of ≥ 10 focal lesions negatively predicted for overall response ($p < 0.05$; OR 4.8). The CT component improved the diagnostic performance of PET.

Conclusion This study showed, for the first time, that cPC morphology and markers related with MM biology, correlate with SUVmax pelvis/liver index, which could be used as a surrogate marker for BM assessment and disease prognosis; PET patterns correlate with MM prognostic features and response rates.

Keywords Multiple myeloma · [18F]-FDG · PET/CT · Plasma cell morphology · Prognostic markers

This article is part of the Topical Collection on Hematology

✉ A. Paschali
anna.pashali@gmail.com

[1] Department of Nuclear Medicine, Theagenion Cancer Hospital, Thessaloniki, Greece

[2] Department of Hematology, Theagenion Cancer Hospital, Thessaloniki, Greece

[3] Hematology/Flow cytometry Lab, Theagenion Cancer Hospital, Thessaloniki, Greece

[4] Hematopathology Department, Evangelismos General Hospital, Athens, Greece

[5] Hematology Department, "St Savvas" Oncology Hospital, Athens, Greece

[6] Department of Clinical Therapeutics, National and Kapodistrian University of Athens, School of Medicine, Athens, Greece

Introduction

Multiple myeloma (MM) is a clonal plasma cell malignant neoplasm that accounts for approximately 10% of hematologic malignant disorders and displays significant genetic, biological, and clinical heterogeneity [1, 2]. The diagnostic armamentarium has significantly expanded in the last decade with contemporary laboratory, molecular, and imaging modalities that deepened our understanding in disease pathology and call for an update on the specific diagnostic criteria and prognostic indices [2].

[18F]-fluoro-deoxy-glucose positron emission tomography/computed tomography ([18F]-FDG PET/CT) is a hybrid imaging modality combining [18F]-FDG PET/metabolic information with a low-dose CT/anatomic information which has become a standard technique in the diagnosis and management of several

types of tumors, particularly in hematology for FDG-avid lymphomas [3]. Recently [18F]-FDG PET/CT has been incorporated in the revised International Myeloma Working Group (IMWG) diagnostic criteria for the assessment of bone disease and it is considered as an essential imaging modality for the recognition of symptomatic MM patients requiring treatment [4].The main strengths of [18F]-FDG PET/CT in MM include the capacity for whole-body imaging, the relatively high sensitivity and specificity for detecting both skeletal/medullary and extramedullary lesions, and the ability to distinguish metabolically active from inactive disease; all these properties have established it as the preferred method of therapy response evaluation and as an essential part of minimal residual disease assessment [4–6]. Furthermore, another important advantage of PET is the potential of quantification of tracer uptake by means of the index standardized uptake value (SUV), which reflects the amount of tracer activity in a particular region of interest, aiding in the objective interpretation of PET/CT scans.

In the context of the newly diagnosed MM (NDMM) patients, [18F]-FDG PET/CT can assess skeletal/medullary and extramedullary disease burden. There have been described four [18F]-FDG PET skeletal patterns: diffuse bone marrow (BM) uptake, focal uptake (with underlying lysis or not), mixed (diffuse +focal), and normal pattern [7]. The prognostic significance of the number of focal lesions in the PET/CT, as well as the identification of extramedullary disease, has been demonstrated in several studies [8–12]. Regarding the diffuse BM [18F]-FDG PET pattern, there is a gray zone of diagnostic uncertainty between the BM reactive changes and the diffuse BM infiltration, and magnetic resonance imaging (MRI) is currently considered the imaging gold-standard method for the detection of diffuse BM involvement [5]. Regarding the normal PET pattern, it is known that in ~ 11% of cases, this is false negative, probably associated with low expression of hexokinase-2 (HK2) [13, 14], but interestingly, this is associated with relatively better prognosis in NDMM patients, as demonstrated in a recent study [14].

Several clinical and biological factors such as age, renal function, cytogenetic abnormalities, MM staging, lactate dehydrogenase (LDH), β2 microglobulin (β2M), circulating plasma cells, and extramedullary involvement correlate with clinical outcomes and are widely used for prognostication in MM [15]. Additionally, clonal plasma cells (cPCs), BM infiltration rate, and cPC morphology have been demonstrated to be independent prognostic factors for survival in MM [16, 17].

Driven from the above and from our observation of significant PET skeletal pattern heterogeneity and the lack of standardization of diffuse BM [18F]-FDG uptake pattern among patients with similar cPC infiltration rates, we designed a prospective study aiming at the investigation of different PET skeletal patterns and the semi-quantitative assessment of non-focal BM [18F]-FDG uptake in the pelvis, in accordance with parameters reflecting disease burden, factors related to disease biology, and finally, response to therapy.

Patients and methods

Patients

In this prospective study, we included 60 NDMM patients and 30 relapsed/refractory MM patients (RRMM) having received one previous line of therapy. The recruitment period started on the 1st of January 2019, the last evaluated patient was enrolled on April 2020, and the study is still ongoing. All patients underwent [18F]-FDG PET/CT scan and BM aspirates of the iliac crest within a period of 2 weeks. Relapsed patients were regarded as eligible if they were off therapy for at least a month prior to the PET/CT scan. All patients received novel agent-based anti-myeloma therapy and they were considered eligible for response evaluation if they had received at least 4 cycles of treatment. Myeloma diagnosis and treatment response were assessed using IMWG criteria [4, 6]; patients with an active infection, concomitant liver, or skeletal-rheumatoid disease at the time of the evaluation were excluded. None of the patients had received growth factors or steroids within 15 days around the PET/CT examination.

Methods

Evaluation of patients'- and disease-related parameters

Demographic, clinical, and laboratory data were collected at the time of imaging examination; these included age, performance status, type of MM, cPC infiltration rate, hemoglobin (Hb) platelets (PLT), serum creatinine and estimated glomerular infiltration rate (eGFR), β2M, LDH, serum calcium, albumin, and ferritin. International staging system (ISS) and revised international staging system (RISS) were also determined. In addition, molecular abnormalities such as t(4;14), t(14;16), t(11;14), deletion 17p (del17p), and 1q gain (1q+) were detected by fluorescent in situ hybridization (FISH).

[18F]-FDG PET/CT methodology and evaluation

All patients underwent whole-body [18F]-FDG PET/CT (from vertex to toes, arms alongside the body) using a time-of-flight LSO PET/16-slice CT scanner (Discovery 710; GE Healthcare, Milwaukee, WI, USA), 50–70 min after IV administration of 3.7 MBq/kg of FDG (maximum dose = 410 MBq). Patients fastened for at least 6 h before injection and were hydrated orally. A whole-body low-dose CT scan was obtained initially at 120 kV, a tube current of 60 mA, tube rotation of 0.8 s, slice thickness of 3.75 mm, 512 × 512 matrix, a 50 cm field of view (FOV), and pitch of 1.375:1, without an

oral or IV contrast agent. Immediately after CT acquisition, whole-body PET emission scans were acquired with a 70 cm axial FOV acquired in three-dimensional mode with a 256 × 256 matrix. A specific iterative CT reconstruction with slice thickness = 1.25 mm was obtained for skeleton evaluation. Iterative image reconstruction for PET was completed with an ordered-subset expectation maximization algorithm (OSEM) (2 iterations, 24 subsets). The blood glucose level required prior to FDG administration was set to ≤ 200 mg/dL.

Whole-body [18F]-FDG PET and low-dose CT part of the studies were evaluated visually by two nuclear medicine physicians, blinded to clinical results, according to IMPeTUs criteria: BM metabolic state, number and site of focal lesions on PET (with or without underlying osteolysis), number of lytic lesions on CT, presence and site of extramedullary or paramedullary disease, and presence of fractures [18]. Diffuse [18F]-FDG uptake in the BM of the axial and the appendicular skeleton was estimated in all patients and was scaled according to the Deauville scoring system (DS) as per the IMPeTUs criteria [18]. Furthermore, for each patient, we calculated the ratio SUVmax pelvis/liver: using a free hand region of interest (ROI) in the central portion of the liver far away from its edge, and another free hand ROI within the pelvis (to include sacrum/L5 and iliac crests) taking care not to include focal areas or other abnormality. Pelvis was selected because this anatomic area is used for diagnostic BM biopsies/aspirates.

We scrutinized the long bones of the limbs (particularly the femurs and the humeri) for the presence or not of hyperdense abnormalities in the medullary cavity in the low-dose CT part of the study, as the recent recommendations by the IMWG Bone Working Group [19], along with the presence or not of diffuse, heterogeneous, or focal FDG uptake in the BM: its extent along the diaphysis as well as the degree of uptake compared to the axial skeleton, by visual evaluation. As the BM of appendicular skeleton is usually replaced by adipose tissue in normal adults [20, 21], we considered positive for diffuse limbs' involvement the cases where there was diffuse or heterogeneous FDG uptake, of various degrees, extending to ≥ than two-thirds of the diaphysis corresponding to hyperdense abnormalities in the medullary cavity in the low-dose CT part of the study. Although no established consensus currently exists on the optimal cutoff density values of the myeloma deposits, medullary lesions in appendicular skeleton with Hounsfield unit > 0 were considered as abnormal [22].

Patients were classified in four PET skeletal patterns: diffuse, focal, mixed (diffuse and focal), and normal. The diffuse pattern was defined as the presence of homogeneously increased [18F]-FDG uptake in the axial skeleton and the pelvis, with or without diffuse limbs' marrow involvement. In the diffuse pattern, we also included cases with diffuse limbs' marrow involvement as defined above, regardless of the intensity of uptake in the axial skeleton [12]. The focal pattern was defined by the existence of one or more foci of increased [18F]-FDG uptake in the skeleton as compared to surrounding normal marrow activity with or without underlying lytic lesions on CT; if osteolysis was not present, the focal lesion should be detectable in at least two adjacent slices; excluded lesions were those related to fractures or joint surface. In patients with focal lesions, the SUVmax of the hottest lesion was recorded. Mixed pattern was defined by the presence of the criteria defining both focal and diffuse pattern. Normal pattern was defined as neither of the above.

Clonal plasma cell morphology assessment

Clonal plasma cell BM infiltration rate and morphology were evaluated by two independent hematologists. To define plasma cell maturation in a uniform fashion, we used the following criteria [17]: (i) presence of nucleoli, (ii) blastic chromatin, and (iii) increased nucleus/cytoplasmic ratio; cPCs which displayed at least two criteria were characterized as intermediate/low differentiated, whereas cPCs with none or one criterion were characterized as well differentiated. Based on the above, we divided patients into 2 groups, those with predominately intermediate/low-differentiated cPCs vs. patients with predominately well-differentiated cPCs.

Statistical analysis

Comparisons were performed with Mann-Whitney U test, X^2 test, and one-way ANOVA. Correlations were performed by Pearson's test. To determine the optimum cutoff value for [18F]-FDG BM uptake positivity, we created a receiver operating characteristic curve (ROC curve) using as state variable the ratio SUVmax pelvis/mediastinum ratio. Likewise, a ROC curve was performed to determine the optimum cutoff value for SUVmax of pelvis, using as state variable SUVmax of mediastinum. Binary logistic regression analysis was used to determine prognostic factors for response. The statistical significance boundary was set to 5%. Data processing and analysis were carried out with the software package SPSS v16.

Results

Patients' characteristics

Ninety patients (M/F: 48/42) with symptomatic MM were included in the study (median age 65 years, range 38–85); 47 patients had IgG MM, 16 had IgA MM, and 21 light chain MM; 2 patients had IgD, IgM, and non-secretory MM, respectively. According to ISS, patients were stratified as follows: ISS1 48, ISS2 16, ISS3 26. High-risk molecular cytogenetics including t(4;14), t(14;16),del17p, and 1q+ were observed in 44% of patients and t(11;14) was detected in 21% of patients;

61 patients (68%) had well-differentiated cPCs and 29 patients (32%) had intermediate/low-differentiated cPCs. Overall, patients' characteristics and type of therapy applied are shown in Table 1.

PET/CT: Qualitative and semi-quantitative evaluation

Patterns of skeletal [18F]-FDG uptake were distributed as follows: diffuse in 15 patients, diffuse + focal in 28 patients, focal in 20 patients, and normal in 27 patients. The median value and the range of the ratio SUVmax pelvis/liver was 1.0 (0.5–7). Distribution according to DS was as follows: DS2 13, DS3 44, DS4 26, DS5 7. Regarding BM metabolic state, there was a good concordance between the classification of the patients as per DS and the value of the ratio SUVmax pelvis/liver ($p < 0.001$). Specifically, 50 patients had SUVmax pelvis/liver < 1.1 and were classified DS 2 ($n = 13$) and 3 ($n = 37$), and 40 patients had SUVmax pelvis/liver ≥ 1.1 and were classified DS 3 ($n = 7$), 4 ($n = 26$), and 5 ($n = 7$). All the patients classified in the diffuse pattern together with 25 out of 28 patients classified in the mixed pattern presented with concomitant diffuse limbs' 18F-FDG marrow uptake, which involved femurs + humeri in 21 patients, femurs only in 13 patients, humeri only in one patient, and femurs + humeri + tibia in 5 patients. Using visual evaluation, the degree of [18F]-FDG uptake in limbs' marrow was similar with the axial skeleton in 30 out of 40 patients with diffuse pattern, lower in 5 patients and higher in 5 patients. In 16 cases, limbs' appearances in both PET and the CT part of the study were helpful to assign these patients in the diffuse pattern, despite the fact that they presented low-grade FDG uptake in the BM of the axial skeleton and pelvis (median ratio SUVmax pelvis/liver = 1.0, range 0.7–1.1). For patients with focal lesions (focal and mixed patterns), the median value and range of SUVmax of focal lesions was 8.1 (2.3–31.0); 31% of patients displayed plasmacytomas (bone-derived = 26, extramedullary = 6). Overall, PET/CT parameters are shown in Table 2; characteristic examples of PET patterns are shown in Fig. 1.

Correlations of PET/CT findings with MM parameters

There was a significant difference in the degree of [18F]-FDG BM uptake in the pelvis as semi-quantified with the ratio SUVmax pelvis/liver, between the two morphology groups: the group of well cPC differentiation demonstrated significantly lower value for the SUVmax ratio pelvis/liver compared to the group of intermediate/low differentiation ($p < 0.001$) (Fig. 2). The median value and the range of the ratio SUVmax pelvis/liver was 0.9 (95% CI 0.6–1.2) in the

Table 1 Patients' characteristics

Variable	Median (range)
Age	65 (38–85)
Sex	M 48, F42
Line of therapy	1st 60, 2nd 30
Treatment	PI-based 76%, Len-based 24%,
M-Component	IgG 47, IgA 16, LC 21, IgD 2, IgM 2, NS 2
ISS	ISS1 48. ISS2 16, ISS3 26
RISS	RISS1 36, RISS2 38, RISS3 14, NA 2
Hb (g/dL)/Hb < 10 g/dL	11.5 (6.0–16.1)/25%
PLT ($\times 10^3/\mu L$)	217 (40–550)
Creatinine (mg/L)	0.8 (0.46–6.6)
B2 microglobulin (mg/L)	3.45 (1.5–52)
Calcium (mg/dL)	9.4 (7.1–13.3)
Albumin (g/dL)	4.1 (2.6–5.9)
LDH (U/L)	19. (91–1604)
Ferritin (ng/mL)	166 (9–794)
BM infiltration (%)	48 (8–99)
Good vs. interm/low differentiation cPCs	61 vs. 29
Molecular cytogenetics: high risk*/del17p/t (11;14)	44%/16%/21%

M, male; *F*, female; *PI*, proteasome inhibitors; *Len*, lenalidomide; *Mo-component*, monoclonal component; *LC*, light chains; *NS*, non-secretory; *ISS*, international staging system; *RISS*, revised ISS; *Hb*, hemoglobin; *PLT*, platelets; *LDH*, lactate dehydrogenase; *BM*, bone marrow; *interm*, intermediate; *cPCs*, clonal plasma cells; *del17p*, deletion 17p

*High risk includes del17p, t(4;140, t(14;16), 1q+

Table 2 PET/CT parameters

Variable	Results
Pattern of 18F-FDG uptake	Diffuse ($n = 15$)
	Diffuse + focal ($n = 28$)
	Focal ($n = 20$)
	Normal ($n = 27$)
BM 18F-FDG uptake median (range)	1.0 (0.5–7.0)
Focal SUVmax	8.1 (2.3–31.0)
Lytic lesions	No. of patients
0	27
1–3	9
4–10	13
> 10	41
Focal lesions	No. of patients
0	42
1–3	12
4–10	12
> 10	24
Appendicular involvement	41 pts
Plasmacytomas (31 pts)	Paramedullary ($n = 26$)
	Extramedullary ($n = 6$)

group of good differentiation vs. 1.2 (95% CI 0.7–7) in the group of intermediate/low differentiation ($p < 0.001$). A characteristic example between two patients with similar infiltration rate but with different BM metabolic state and plasma cell morphology is shown in Fig. 3; [18F]-FDG BM uptake correlations as semi-quantified with the ratio SUVmax pelvis/liver are shown in Table 3. SUVmax pelvis/liver ratio showed a moderate positive correlation with cPC infiltration rate (Fig. 4), β2M, and serum ferritin, and also a positive correlation with ISS and RISS (Table 3); particularly, patients with advanced stage (ISS3 or RISS3) had significantly a greater value SUVmax pelvis/liver compared to ISS1/2 or RISS1/2, respectively (Table 3). Importantly, there was no significant correlation between the value SUVmax pelvis/liver and Hb (Table 3).

Regarding the cutoff level of the ratio SUVmax pelvis/liver, a ROC curve demonstrated that 1.1 displays excellent specificity (99%) and good sensitivity (76%) for diffuse BM involvement (AUC 0.94; $p < 0.001$), whereas a ROC curve cutoff value of ≥ 3.35 for the SUVmax of pelvis displayed sensitivity 71% and specificity 67% (AUC 0.75; $p < 0.001$). Deauville score 4 and 5 confirmed a positive correlation with dismal prognostic markers such as β2M, LDH, high BM infiltration, poor differentiation morphology, and advanced ISS and RISS stage ($p < 0.05$ for all parameters).

Distribution of patterns of [18F]-FDG uptake among studied patients is depicted in Table 2. Diffuse pattern correlated with standard risk molecular profile ($p < 0.05$); mixed pattern correlated with poor prognostic features such as high β2M, high BM infiltration rate, and intermediate/low differentiation cPC morphology ($p < 0.05$ for all parameters); focal pattern correlated with low infiltration rate (< 20%, $p < 0.05$). An appreciable percentage of patients (30%) displayed normal PET pattern which correlated with good prognostic MM features such as good differentiated cPCs (82% of patients), and low β2M. Interestingly, t(11;14) was present in 37% of patients with normal pattern vs. 13% of patients with other patterns of [18F]-FDG uptake ($p = 0.01$). In addition to the different patterns of [18F]-FDG uptake, appendicular involvement (diffuse or mixed) correlated with adverse MM prognostic factors such as advanced RISS, higher β2M and LDH, and intermediate/low-differentiated cPC morphology ($p < 0.05$).

Prognostic factors for response to anti-myeloma therapy

Eighty-two patients were evaluated for response; overall response rate (ORR) was 79% (complete response 30%, very good partial response 18%, partial response 30%, stable disease 16%, and progressive disease 6%). In the univariate binary logistic regression analysis mixed PET/CT pattern, appendicular BM involvement, presence of ≥ 10 focal lesions, and treatment with proteasome inhibitor-based regimens predicted for ORR ($p < 0.05$ for all parameters; odds ratio 3.7, 3.3, 4.8, and 4.0 respectively); at variance, disease-related parameters such as age, BM infiltration, β2M, LDH, ISS, and RISS did not display prognostic impact on response. In the multivariate analysis, presence of ≥ 10 focal lesions and treatment with proteasome inhibitor-based regimens were the most powerful prognostic parameters for ORR ($p < 0.05$; odds ratio 4.8 and 4.1, respectively).

Discussion

The aim of the current study was to examine the diagnostic value of a semi-quantitative method for the evaluation of non-focal FDG uptake in pelvis, which is the anatomic area used for the performance of BM aspiration or biopsy, to describe PET/CT skeletal patterns of the disease and to correlate PET/CT findings with parameters reflecting tumor burden, disease biology, and response to therapy.

We showed that BM [18F]-FDG uptake in the pelvis, expressed as the ratio SUVmax pelvis/liver, correlates significantly with cPC morphology, adding thus, for the first time to the best of our knowledge, a novel information about the link between advanced imaging and cPC biology. In particular, the group of patients with well-differentiated cPCs had significantly less [18F]-FDG uptake in the pelvis compared to the intermediate/low differentiation group. The exact etiology of

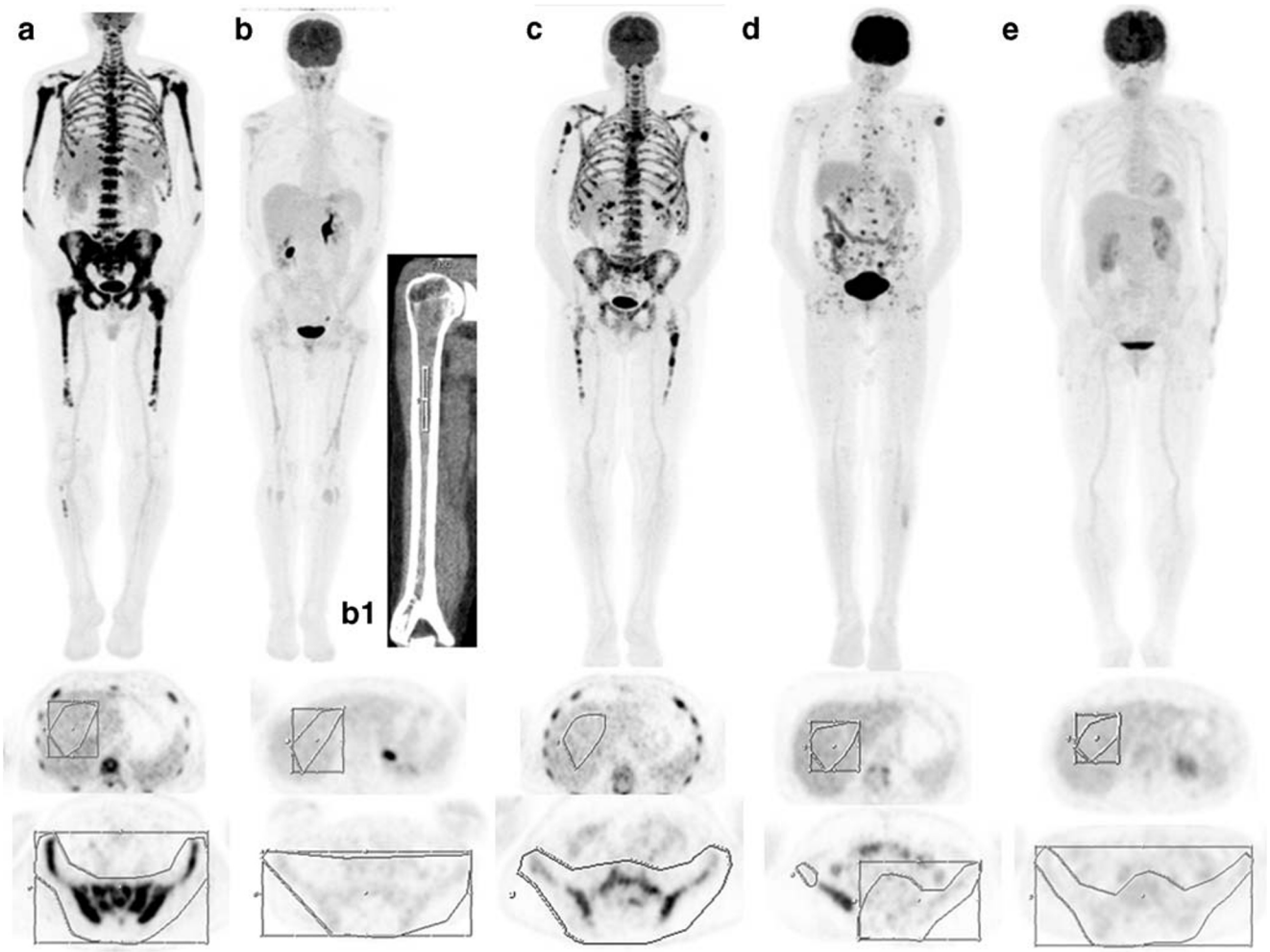

Fig. 1 Typical examples of each of the patterns: MIP (Maximum Intensity Projection), as well as the axial PET slices of the pelvis and the liver showing the ROIs used for the SUVmax pelvis/liver ratio: **a** Diffuse pattern with diffusely increased 18F-FDG uptake in the axial and appendicular skeleton (SUVmax pelvis/liver = 5.4, IMPeTUs: BM-DS5-A, F1, L4, EM-EN-other). This is a NDMM patient with 83% medullary infiltration by poorly differentiated cPCs. **b** Diffuse pattern with diffuse limbs' marrow 18F-FDG uptake (femurs, humeri, tibia) and marginal axial 18F-FDG uptake (SUVmax pelvis/liver = 1.1, IMPeTUs:BM-DS4-A). This is a NDMM patient with 58% medullary infiltration by well-differentiated cPCs. **b1** Sagittal cut of the low-dose CT part shows diffuse hyperdense abnormalities in the medullary cavity of the humerus (HU = 85)**. c** Mixed pattern with diffuse and focal 18F-FDG uptake in the axial and appendicular skeleton (SUVmax pelvis/liver = 4.6, IMPeTUs: BM-DS5-A, F4-DS5-Sp-EXSP, L4, Fr). This is a relapsed patient with 46% medullary infiltration by poorly differentiated cPCs. **d** Focal pattern with multiple foci of increased 18F-FDG uptake in the axial and appendicular skeleton and no diffuse BM uptake (SUVmax pelvis/liver = 0.8, IMPeTUs: BM-DS3, F4-DS5-Sp-EXSP, L4, Fr). This is a relapsed patient with 25% medullary infiltration by well-differentiated cPCs. **e** Normal pattern in a NDMM patient with 69% medullary infiltration by well-differentiated cPCs (SUVmax pelvis/liver = 0.9, IMPeTUs: BM-DS3). BM-DS, diffuse bone marrow Deauville score; F, focal bone lesions—numbers according to IMPeTUs criteria [19]; L, lytic lesions on CT—numbers according to IMPeTUs criteria; EM-EN-other, extramedullary disease-extranodal-other; SP, spine; EXSP, extra-spine

this correlation is not clear; however, a possible explanation could be that low-differentiated cPCs may have increased metabolic activity expressed by increased glycolytic rate per se, or create a more metabolically active microenvironment in the BM compared to the infiltration by mature cPCs; indeed, there was a positive correlation of BM [18F]-FDG uptake with CD45 expression in cPCs (data not shown), which is a marker reflecting cPCs' proliferative rate [23]; nonetheless, currently, there is no experimental proof on the above hypothesis. Moreover, we found positive correlation of BM [18F]-FDG uptake expressed as the ratio SUVmax pelvis/liver, with parameters reflecting disease burden (BM infiltration rate, and β2M) as well as with serum ferritin which reflects disease activity [24]. Sachpekidis et al, using dynamic FDG PET of the lower lumbar spine and pelvis, demonstrated positive correlation between BM infiltration rate with [18F]-FDG kinetic parameters (Ki, influx, fractal dimension) and SUV average of the pelvis [7]. However, dynamic PET is a time-consuming and elaborate process, not routinely performed in everyday clinical practice, whereas our proposed BM [18F]-FDG uptake index is a more practical means of estimating BM involvement.

Table 3 Correlations of SUVmax pelvis/liver

Variable	NS
Hb	NS
LDH	NS
Albumin	$r = 0.4$ ($p < 0.001$)
B2M	$r = 31$ ($p = 0.01$)
Ferritin	1.2 (0.8–6.3) vs. 1.0 (0.6–7.0) $p = 0.001$
ISS3 vs. ISS1/2	1.2 (0.7–6.3) vs. 0.9 (0.5–7.0) $p = 0.007$
Pts with Del17p vs. others	NS
High-risk molecular cytogenetics*	NS
t(11;14)	0.9 (0.9–2.5) vs. 1.1 (0.6–7.0) $p = 0.01$
BM infiltration (10%)	$r = 0.32$ ($p = 0.002$) (pos)
cPCs morphology (good vs. intermediate/low differentiation)	0.9 (0.6–1.2) vs. 1.2 (0.7–7.0, $p < 0.001$)

B2M, β2 microglobulin; *LDH*, lactate dehydrogenase; *ISS*, international staging system; *RISS*, revised ISS; *del17p*, deletion 17p; *BM*, bone marrow

*High risk includes del17p, t(4;140, t(14;16), 1q+

Of note, in our study, there was no significant correlation between the ratio SUVmax pelvis/liver and hemoglobin levels. Anemia (Hb < 10 g/dL) was present in 25% of patients; however, these patients did not exhibit higher diffuse BM [18F]-FDG uptake compared to the others. It is known that PET/CT accuracy for BM assessment may be compromised by erythroblastic rebound due to anemia [18]. However, this is not the case in MM, considering that the erythroid cell compartment that could probably contribute to false positive diffuse BM [18F]-FDG uptake is reduced in MM, due to BM infiltration and to mechanisms involved in anemia of MM that is anemia of chronic disease [25].

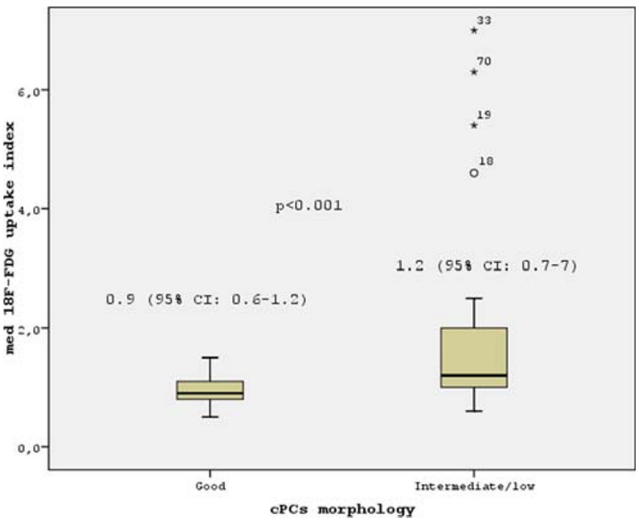

Fig. 2 This graph shows the significant difference of the median value of 18F-FDG BM uptake in the pelvis as semi-quantified with the ratio SUVmax pelvis/liver, as well as all the values of the group with good and the group with intermediate/low, the box with the median and IQR values, and the outlier values

Regarding patterns of BM [18F]-FDG uptake, the majority displayed a mixed pattern (28/90 patients), which correlated with higher rate of BM infiltration, confirming previous findings by Sachpekidis et al. [7]. In addition, we showed that mixed pattern correlated with higher β2M and intermediate/low-differentiated cPC morphology, suggesting that there is a distinct disease biology related to this pattern of BM [18F]-FDG uptake.

An appreciable percentage of patients in our study (30%) displayed normal PET pattern, which was correlated with good prognostic features such as mature cPC morphology, low β2M, and limited BM infiltration. The quota of normal pattern in our study, which is actually "false negative," is higher compared to two recent studies (~ 11%) that employed both whole-body PET/CT and whole-body MRI in NDMM patients [13, 14]; interestingly, in these studies, the false-negative PET pattern correlated with lower HK2 expression levels, which is known to be related with [18F]-FDG uptake in tumor cells, and was associated with relatively better prognosis [14]. Of note, in another recent study on a small cohort of relapsed patients, the levels of HK2 expression were not lower in the false-negative [18F]-FDG PET patients, which implies that other unknown factors are responsible for this metabolic heterogeneity [26]. Another interesting finding was that 37% of patients with normal pattern displayed t(11;14), a quite common and prognostically neutral molecular abnormality detected by FISH in approximately 15–20% of MM patients [27]; its presence results in upregulation of cyclin D1, the overexpression of which theoretically favors cell cycle progression, as seen in mantle cell lymphoma (MCL) [28]. In MM, t(11;14) has been associated with lymphoplasmacytic morphology and increased numbers of circulating cPCs [29]. In lymphoid malignancies overexpressing cyclin D1 such as MCL, it was demonstrated that sensitivity of [18F]-FDG PET/

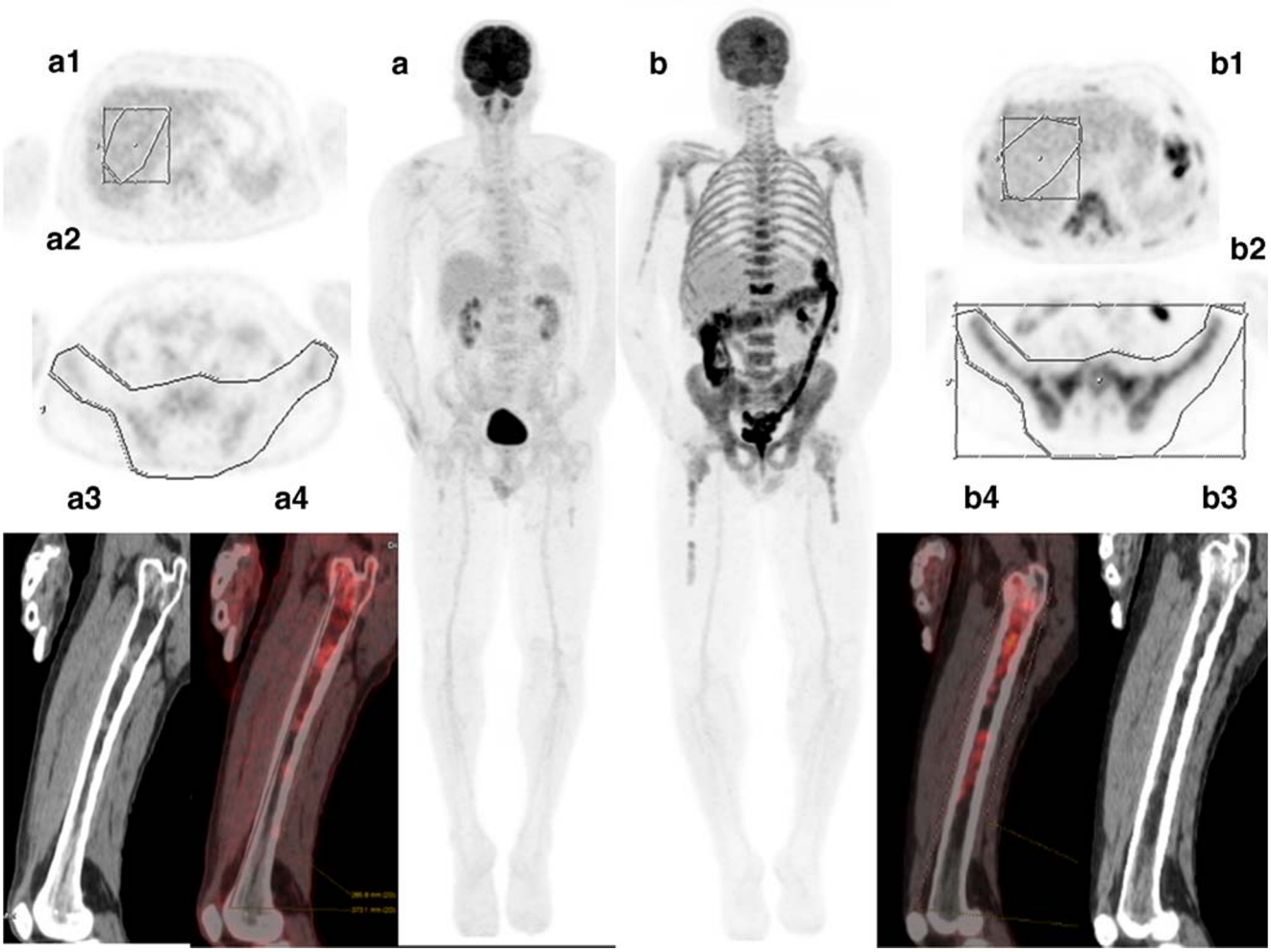

Fig. 3 Characteristic examples of two patients with similar infiltration rate but with different BM metabolic state and different plasma cell morphology. Patient A has 66% infiltration rate of well-differentiated cPCs, while patient B has 60% infiltration rate of poorly differentiated cPCs. MIP (maximum intensity projection), axial PET slices of liver and pelvis showing ROIs used for the SUVmax pelvis/liver ratio and sagittal PET and CT slices of the femurs are shown. Patient A has a SUVmax pelvis/liver ratio = 1.1 while patient B SUVmax pelvis/liver ratio = 2.4. Patient A is a characteristic example of low FDG BM metabolic state in which CT helps to assign this patient in the diffuse pattern, as it shows dense BM abnormalities in the medullary cavity of the femurs

CT in detecting BM infiltration is extremely low, suggesting a low metabolic activity of MCL lymphocytes in the BM [28]. Likewise, cPCs with t(11;14) overexpressing cyclin D1 may also exhibit low proliferative rate resembling that of normal plasma cells as previously suggested [27]. Consequently, the normal [18F]-FDG PET pattern consists an appreciable percentage of MM patients, associated with disease features related with good prognosis; however, further investigation is needed along with the application of new tracers targeting different metabolic pathways or receptors expressed by cPCs.

The use of the ratio SUVmax pelvis/liver follows the same rational as the DS, which is incorporated in the IMPeTUs criteria [18, 30, 31], however, taking a standard reference area (pelvis), in contrast to the visual selection of the BM macro area in the IMPeTUs criteria, which depends on the observer's experience. Our study displayed a very good concordance between the proposed index and the DS. Indeed, there were only 7 cases with marginal BM metabolic state, in which the proposed index SUVmax pelvis/liver was indicative for BM positivity, although classified as DS3. Since normal pelvic FDG uptake is generally lower than hepatic uptake, the ratio SUVmax pelvis/liver provides an absolute number, which is partially free from factors that influence SUV, such as patient weight. Furthermore, this index estimates the [18F]-FDG uptake combining parts from the axial and appendicular skeleton, as the sacrum and lumbar-5 vertebra belong to the axial skeleton and the iliac bones to the appendicular skeleton. Regarding correlations of Deauville 5-scale evaluation with MM parameters, only advanced score (4 or 5) correlated significantly with important markers reflecting disease activity including β2M, LDH cPC morphology, and advanced RISS; on the other hand, ratio SUVmax pelvis/liver is a more accurate and suitable method to evaluate BM [18F]-FDG uptake; a ROC curve demonstrated that BM uptake ≥ 1.1 displays an 99% specificity and a 76% sensitivity and may be used to define

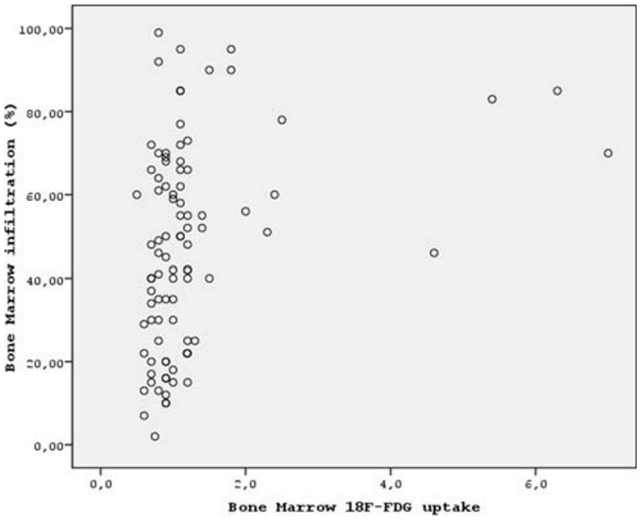

Fig. 4 This graph shows the moderate positive correlation between the ratio SUVmax pelvis/liver and BM cPC infiltration rate ($p = 0.002$, $r = 0.32$)

[18F]-FDG BM uptake positivity. Although no positivity cutoff for the BM metabolic state has been set by the IMPeTUs criteria at the phase of the initial diagnosis or at the recurrence, our cutoff value for the ratio SUVmax pelvis/liver ≥ 1.1 equals to > liver uptake + 10% which corresponds to DS 4 and 5, and could be ancillary applied in MM and used as a marker reflecting tumor burden and cPC metabolic activity. Interestingly, DS 4 and 5 were set posteriori, as positivity cutoffs in a large and homogeneous patient population (228 pts) evaluated with [18F]-FDG PET/CT before therapy and pre-maintenance in the light of follow-up data [32]. This study concludes that patients who maintain a DS ≥ 4 in the BM have a significantly shorter progression-free survival (PFS) and a significantly shorter overall survival (OS) [32]. In addition, in a recent study, it was shown that Durie–Salmon Plus stage III based on IMPeTUs and the DS of BM ≥ 4 were reliable prognostic factors, associated with OS, in NDMM patients [33]. Among the several other methods that have been proposed for quantifying the extent of disease in MM patients such as total lesion glycolysis (TLG), metabolic tumor volume (MTV) [34, 35], and intensity of bone involvement (IBI) [36], none intended to measure diffuse BM uptake alone, while a number of methodological issues limit their application in clinical practice.

In our study, 41 patients demonstrated appendicular involvement in the PET and the CT part of the study. Appendicular involvement has been recognized as an unfavorable prognostic factor in NDMM patients, in several studies employing [18F]-FDG PET/CT [37] or whole-body low-dose CT [38, 39]. Particularly in the recent study by Abe Y et al. in NDMM patients with high-risk factors, it was shown that the presence of more than three focal lesions in the appendicular skeleton on [18F]-FDG PET/CT was an independent negative predictor of survival and was significantly associated with advanced disease stage, high-risk cytogenetics, and high tumor burden [37]. Our study confirmed that appendicular involvement correlated with adverse MM prognostic factors such as advanced RISS, higher β2M, and intermediate/low-differentiated cPC morphology. Furthermore, patients who displayed appendicular involvement had almost 4-fold probability to fail achieving at least PR, indicating that appendicular skeleton involvement may offer important prognostic information regarding treatment outcome. Moreover, a careful evaluation of the CT appearances of the long bones may complement and improve not only the prognostic but also the diagnostic performance of PET. Medullary infiltration without osteolysis is very hard to detect in the axial skeleton due to the presence of dense trabecular bone; however, in the appendicular skeleton, this can be depicted in the CT because BM is usually replaced by adipose tissue in adults [19]. Indeed, in our study, appendicular BM abnormalities detected in the CT were indicative of BM infiltration in almost 25% of the patients who exhibited low degree of FDG uptake in the axial and appendicular skeleton, almost non-discerned by non-experienced readers. We set as positive for appendicular involvement the combination of PET and CT parameters in order to increase the specificity, as it is known that not all hyperattenuating medullary regions neither all cases of FDG uptake in the limbs are specific for pathologic BM infiltration; increased red marrow reconversion, either related to chronic causes such as severe anemia, obesity and heavy smoking, or to treatment-induced changes, may also manifest as increased density within the cavities of the proximal long bones [40]. Importantly, appendicular involvement was incorporated in the criteria used to determine diffuse pattern of BM 18F-FDG uptake in the recently published phase 3 collaborative randomized study (IFM/DFCI-2009), underlying the importance of this parameter for the interpretation of PET/CT [12].

Apart from the prognostic significance of appendicular involvement in the multivariate analysis, it was demonstrated that the presence of more than 10 focal lesions was the most powerful parameter for ORR exhibiting a 4-fold higher probability for sub-optimal response; this latter finding confirmed previous reports demonstrating the importance of the presence of focal lesions in MM prognosis [5, 11].

Finally, a possible limitation of our study was the evaluation of patients both at initial diagnosis and at first relapse; this was the reason for not attempting any correlations with PFS or OS; however, taking into account that first and second lines are considered as “early lines” and all patients were treated with highly effective therapies, correlations with ORR were feasible. We are currently continuing to enroll NDMM patients to confirm our results and explore correlations with MM outcomes.

In conclusion, MM presents with significant metabolic heterogeneity, ranging from low to extremely high and the estimation of the BM involvement is limited by the visual evaluation of PET only. The ratio SUVmax pelvis/liver is a simple and practical index of grading the intensity of diffuse BM involvement in MM that correlates with significant disease

burden parameters and cPC morphology; correlations of BM uptake with cPC morphology have been demonstrated for the first time to our knowledge, indicating that this index could serve as a surrogate marker of MM biology. Moreover, PET skeletal mixed pattern correlates with poor MM prognostic features while normal pattern consists an appreciable percentage of MM patients which associates with parameters related with good prognosis. Finally, the CT component of PET/CT could aid the assessment of diffuse infiltration in a significant number of cases with no or low 18F-FDG uptake. More studies are needed to corroborate our findings.

Authors' contributions Conceptualization: Anna Paschali and Eirini Katodritou. PET/CT data collection and analysis: Anna Paschali, Emmanouil Panagiotidis, and Eirini Katodritou. Patient selection, diagnostic procedures, monitoring, and treatment: Eirini Katodritou, Theodora Triantafyllou, Vassiliki Palaska, Kyriaki Tsirou, Evgenia Verrou, Pavlina Konstantinidou, Asimina Papanikolaou, Anastasia Pouli, and Anna Paschali. BM aspiration evaluation: Eirini Katodritou, Theodora Triantafyllou, and Dimitra Markala. MM data collection and data management: Eirini Katodritou and Theodora Triantafyllou. Flow cytometry/BM evaluation: Efthalia ϒiannaki, Dimitra Markala, Eirini Katodritou, and Theodora Triantafyllou. Investigation: Anna Paschali, Eirini Katodritou, Evangelos Terpos, Theodora Triantafyllou, Vasiliki Chatzipavlidou, and Emmanouil Panagiotidis. Statistical analysis: Eirini Katodritou. Writing-original draft preparation: Anna Paschali and Eirini Katodritou. Review and editing of the paper: Eirini Katodritou, Evangelos Terpos, Emmanouil Panagiotidis, and Anna Paschali.

Data availability The datasets generated during and/or analyzed during the current study are available from the corresponding author on reasonable request.

Compliance with ethical standards

Conflict of interest The authors declare that they have no conflict of interest.

Ethics approval The study was conducted, in accordance with the ethical principles laid down in the Declaration of Helsinki 2008 revision. The study was approved by the Ethics Committee of Theagenion Cancer Hospital.

Consent to participate Informed consent was obtained from all individual participants included in the study.

Consent for publication Patients signed informed consent regarding publishing their data and images.

References

1. Rajkumar SV. Multiple myeloma: 2018 update on diagnosis, risk-stratification, and management. Am J Hematol. 2018;93:1091–110.
2. Landgren O, Morgan G. Biologic frontiers in multiple myeloma: from biomarker identification to clinical practice. Clin Cancer Res. 2018;20:804–13.
3. Cheson BD, Fisher RI, Barrington SF, Cavalli F, Schwartz LH, Zucca E, et al. Recommendations for initial evaluation, staging, and response assessment of Hodgkin and non-Hodgkin lymphoma: the Lugano classification. J Clin Oncol. 2014;32:3059–68.
4. Rajkumar SV, Dimopoulos MA, Palumbo A, Blade J, Merlini G, Mateos MV, et al. International myeloma working group updated criteria for the diagnosis of multiple myeloma. Lancet Oncol. 2014;15:538–48.
5. Cavo M, Terpos E, Nanni C, Moreau P, Lentzsch S, Zweegman S, et al. Role of 18F-FDG PET/CT in the diagnosis and management of multiple myeloma and other plasma cell disorders: a consensus statement by the International Myeloma Working Group. Lancet Oncol. 2017;18:206–17.
6. Kumar S, Paiva B, Anderson KC, Durie B, Landgren O, Moreau P, et al. International myeloma working group consensus criteria for response and minimal residual disease assessment in multiple myeloma. Lancet Oncol. 2016;17:328–46.
7. Sachpekidis C, Mai EK, Goldschmidt H, Hillengass J, Hose D, Pan L, et al. 18F-FDG dynamic PET/CT in patients with multiple myeloma. Patterns of tracer uptake and correlation with bone marrow plasma cell infiltration rate. Clin Nucl Med. 2015;40:300–7.
8. Aljama MA, Sidiqi MH, Buadi FK, Lacy MQ, Gertz MA, Dispenzieri A, et al. Utility and prognostic value of 18 F-FDG positron emission tomography-computed tomography scans in patients with newly diagnosed multiple myeloma. Am J Hematol. 2018;93:1518–23.
9. Bartel TB, Haessler J, Brown TL, Shaughnessy JD Jr, van Rhee F, Anaissie E, et al. F18-fluorodeoxyglucose positron emission tomography in the context of other imaging techniques and prognostic factors in multiple myeloma. Blood. 2009;114:2068–76.
10. Zamagni E, Patriarca F, Nanni C, Zannetti B, Englaro E, Pezzi A, et al. Prognostic relevance of 18-F FDG PET/CT in newly diagnosed multiple myeloma patients treated with up-front autologous transplantation. Blood. 2011;118:5989–95.
11. Zamagni E, Nanni C, Gay F, Pezzi A, Patriarca F, Bello M, et al. 18F-FDG PET/CT focal, but not osteolytic, lesions predict the progression of smoldering myeloma to active disease. Leukemia. 2016;30:417–22.
12. Moreau P, Attal M, Caillot D, Macro M, Karlin L, Garderet L, et al. Prospective evaluation of magnetic resonance imaging and [18 F]fluorodeoxyglucose positron emission tomography-computed tomography at diagnosis and before maintenance therapy in symptomatic patients with multiple myeloma included in the IFM/DFCI 2009 trial: results of the IMAJEM study. J Clin Oncol. 2017;35:2911–8.
13. Rasche L, Angtuaco E, McDonald JE, Buros A, Stein C, Pawlyn C, et al. Low expression of hexokinase-2 is associated with false negative FDG-positron emission tomography in multiple myeloma. Blood. 2017;130:30–4.
14. Abe Y, Ikeda S, Kitadate A, Narita K, Kobayashi H, Miura D, et al. Low hexokinase-2 expression-associated false-negative 18F-FDG PET/CT as a potential prognostic predictor in patients with multiple myeloma. Eur J Nucl Med Mol Imaging. 2019;46:1345–50.
15. Ziogas D, Kastritis E, Dimopoulos MA. Prognostic factors for multiple myeloma in the era of novel agents. Expert Rev Hematol. 2018;11:863–79.
16. Rajkumar SV, Fonseca R, Lacy MQ, Witzig TE, Therneau TM, Kyle RA, et al. Plasmablastic morphology is an independent predictor of poor survival after autologous stem-cell transplantation for multiple myeloma. J Clin Oncol. 1999;17:1551–7.
17. Goasguen JE, Zandecki M, Mathiot C, Scheiff JM, Bizet M, Ly-Sunaram B, et al. Mature plasma cells as indicator of better prognosis in multiple myeloma. New methodology for the assessment of plasma cell morphology. Leuk Res. 1999;23:1133–40.
18. Nanni C, Zamagni E, Versari A, Chauvie S, Bianchi A, Rensi MF, et al. Image interpretation criteria for FDG PET/CT in multiple myeloma: a new proposal from an Italian expert panel. IMPeTUs

(Italian myeloma criteria for PET USe). Eur J Nucl Med Mol Imaging. 2016;43:414–21.
19. Moulopoulos LA, Koutoulidis V, Hillengass J, Zamagni E, Aquerreta JD, Roche CL, et al. Recommendations for acquisition, interpretation and reporting of whole body low dose CT in patients with multiple myeloma and other plasma cell disorders: a report of the IMWG Bone Working Group. Blood Cancer J. 2018;8:95.
20. Vande Berg BC, Malghem J, Lecouvet FE, Maldague B. Magnetic resonance imaging of the normal bone marrow. Skelet Radiol. 1998;27:471–83.
21. Chan BY, Gill KG, Rebsamen SL, Nguyen JC. MR imaging of pediatric bone marrow. RadioGraphics. 2016;36:1911–30.
22. Horger M, Pereira P, Claussen CD, Kanz L, Vonthein R, Denecke B, et al. Hyperattenuating bone marrow abnormalities in myeloma patients using whole-body non-enhanced low-dose MDCT: correlation with haematological parameters. Br J Radiol. 2008;81:386–96.
23. Pellat-Deceunynck C, Bataille R. Normal and malignant human plasma cells: proliferation, differentiation, and expansions in relation to CD45 expression. Blood Cells Mol Dis. 2004;32:293–301.
24. Papadaki H, Kyriakou D, Foudoulakis A, Markidou F, Alexandrakis M, Eliopoulos GD. Serum levels of soluble IL-6 receptor in multiple myeloma as indicator of disease activity. Acta Haematol. 1997;97:191–5.
25. Katodritou E, Dimopoulos MA, Zervas K, Terpos E. Update on the use of erythropoiesis-stimulating agents (ESAs)for the management of anemia of multiple myeloma and lymphoma. Cancer Treat Rev. 2009;35:738–43.
26. Kircher S, Stolzenburg A, Kortüm KM, Kircher M, Da Via M, Samnick S, et al. Hexokinase-2 expression in 11C-methionine-positive, 18F-FDG-negative multiple myeloma. J Nucl Med. 2019;60:348–52.
27. Fonseca R, Blood EA, Oken AA, Kyle RA, Dewald GW, Baliy RJ, et al. Myeloma and the t(11;14)(q13;q32); evidence for a biologically defined unique subset of patients. Blood. 2002;99:3735–41.
28. Albano D, Treglia G, Gazilli M, Cerudelli E, Giubbini R, Bertagna F, et al. 18 F-FDG PET or PET/CT in mantle cell lymphoma. Clin Lymphoma Myeloma Leuk. 2020;20:422–30.
29. Rajan AM, Rajkumar SV. Interpretation of cytogenetic results in multiple myeloma for clinical practice. Blood Cancer J. 2015;5:365.
30. Nanni C, Versari A, Chauvie S, Bertone E, Bianchi A, Rensi M, et al. Interpretation criteria for FDG PET/CT in multiple myeloma (IMPeTUs): final results. IMPeTUs (Italian myeloma criteria for PET USe). Eur J Nucl Med Mol Imaging. 2018;45:712–9.
31. Nanni C. PET-FDG: Impetus. Cancers (Basel). 2020;12:1030.
32. Zamagni E, Nanni, Dozza L, Carlier, Bailly C, Tacchetti P, et al. Standardization of 18F-FDG PET/CT according to Deauville criteria for metabolic complete response definition in newly diagnosed transplant eligible multiple myeloma (MM) patients: joint analysis of two prospective randomized phase III trials. Blood 2018;132(Supplement 1):257-257. https://doi.org/10.1182/blood-2018-99-111321.
33. Shengming D, Bin Z, Zhou Y, Xu X, Li J, Sang S, et al. The role of 18F-FDG PET/CT in multiple myeloma staging according to IMPeTUs: comparison of the Durie–Salmon plus and other staging systems. Contrast Media Mol Imaging. 2018;2018:4198673. https://doi.org/10.1155/2018/4198673.
34. Fonti R, Larobina M, Del Vecchio S, De Luca S, Fabbricini R, Catalano L, et al. Metabolic tumor volume assessed by 18F-FDG PET/CT for the prediction of outcome in patients with multiple myeloma. J Nucl Med. 2012;53:1829–35.
35. McDonald JE, Kessler MM, Gardner MW, Buros AF, Ntambi JA, Waheed S, et al. Assessment of total lesion glycolysis by 18F FDG PET/CT significantly improves prognostic value of GEP and ISS in myeloma. Clin Cancer Res. 2017;23:1981–7.
36. Takahashi MES, Mosci C, Souza EM, Brunetto SQ, Etchebehere E, Santos AO, et al. Proposal for a quantitative 18 F-FDG PET/CT metabolic parameter to assess the intensity of bone involvement in multiple myeloma. Sci Rep. 2019;9:16429. https://doi.org/10.1038/s41598-019-52740-2.
37. Abe Y, Narita K, Kobayashi H, Kitadate A, Takeuchi M, O'uchi T, et al. Medullary abnormalities in appendicular skeletons detected with 18 F-FDG PET/CT predict an unfavorable prognosis in newly diagnosed multiple myeloma patients with high-risk factors. Am J Roentgenol. 2019;213:918–24.
38. Nishida Y, Matsue Y, Suehara Y, Fukumoto K, Fujisawa M, Takeuchi M, et al. Clinical and prognostic significance of bone marrow abnormalities in the appendicular skeleton detected by low-dose whole-body multidetector computed tomography in patients with multiple myeloma. Blood Cancer J. 2015;5:e329. https://doi.org/10.1038/bcj.2015.57.
39. Matsue K, Kobayashi H, Matsue Y, Abe Y, Narita K, Kitadate A, et al. Prognostic significance of bone marrow abnormalities in the appendicular skeleton of patients with multiple myeloma. Blood Adv. 2018;2:1032–9.
40. Spira D, Weisel K, Brodoefel H, Schulze M, Kaufmann S, Horger M. Can whole-body low dose multidetector CT exclude the presence of myeloma bone disease in patients with monoclonal gammopathy of undetermined significance (MGUS)? AcadRadiol. 2012;19:89–94.